Engineering

Multi-material 3D printing guided by machine vision

Yong Lin Kong

A 3D printer uses machine vision to solve a problem that has plagued 3D inkjet printers, increasing the range of materials that can be used, and enabling the rapid production of complex objects such as a robot hand. **See p.522**

Advances in additive manufacturing, also known as 3D printing, have generated increasingly powerful capabilities for producing geometrically complex structures that could not be made using conventional manufacturing processes. However, seamlessly integrating different materials into a single high-resolution 3D-printing process remains a challenge, especially for materials that have disparate properties. On page 522, Buchner *et al.*[1] report a 3D-printing platform that can rapidly adapt its printing parameters in real time by acquiring topological information about the object being constructed using a powerful machine-vision system. This approach, which the authors call vision-controlled jetting, expands the palette of materials that can be used in inkjet 3D printing, opening the way to the fabrication of geometrically complex, multi-material constructs with high throughput.

3D printing is a broad class of manufacturing technologies in which materials are added together to produce objects, in contrast to conventional processes that work by removing sections from a bulk material (for instance, machining) or re-forming a material (such as moulding). The additive nature of 3D printing provides opportunities to optimize the printed constructs by programming or modulating the properties of materials at the microscopic level – for example, by tuning the processing conditions or by integrating other materials. In the past few years, machine vision[2] and artificial intelligence[3] have also been incorporated into 3D-printing processes to sense and adapt the printing environment and thereby automate the printing optimization process.

Material jetting is a class of 3D printing that can be used to make multi-material constructs at micrometre-scale resolution. It works by printing a liquid resin material through hundreds to thousands of individually controllable nozzles. In one of the most common types of machine jetting, the deposited resin sets hard (cures) when it is irradiated with ultraviolet light, therefore allowing a 3D object to be built up layer by layer.

A limitation of material jetting is that the thickness of each printed layer is not perfectly uniform, as a result of intrinsic variations in droplet volume caused by variable flow rates, interference between jetted droplets from individual nozzles and shrinkage of cured printed droplets. Without adjustment, any irregularities stack up with those in subsequent layers, which can lead to defects in the resulting object and ultimately print failure. A process known as mechanical planarization is therefore required, in which a blade or roller levels the printed feature to its expected thickness before the next layer is printed. However, mechanical planarization limits the range of materials that can be printed, because only those that are compatible with the scraper or roller can be used – preventing the use of many polymers that have more-suitable properties for consumer and industrial products.

To solve this problem, Buchner *et al.* developed a material-jetting 3D printer that integrates a machine-vision system, composed of four cameras and two laser sources, to scan the profile of printed layers. This contactless scanning acquires topological information at microscale resolution (down to a volume of 64 μm × 32 μm × 8 μm). This is not the first example of machine vision being integrated into a material-jetting 3D printer[4], but the authors' custom-made system can scan 660 times faster than the one used in the previous work, and the system's graphics-processing unit analyses topological information in less than one second. The scanned profile is then compared with a computer model of the desired construct, and the ink volume of the subsequent layer is adjusted to compensate for any deviations from the model (Fig. 1).

This feedback system eliminates the need for mechanical planarization, allowing the use of resins that would otherwise be incompatible with material jetting – for example, the authors demonstrate that their platform can print certain types of engineering-grade polymer. Moreover, the process enables the use of removable support materials, such as wax, that are needed when producing intricate features. Impressively, structurally complex multi-material constructs can be printed both with high resolution (with a voxel size of 32 μm × 64 μm × 20 μm; a voxel, or volume pixel, is the smallest distinguishable element of a 3D printed object) and high throughput (24 × 10^9 voxels per hour) on a par with current

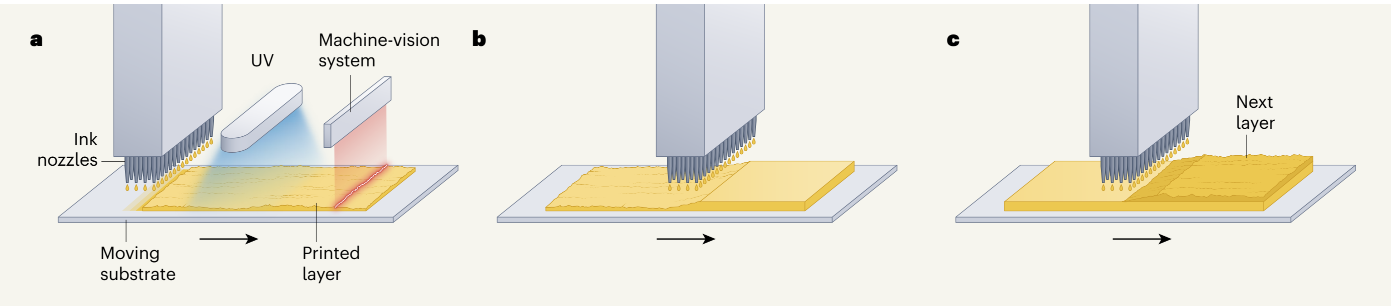

Figure 1 | How machine vision prevents 3D-printing failure. **a**, In the 3D-printing process known as material jetting, a liquid resin is deposited through individually controllable nozzles. The deposited resin sets hard when irradiated with ultraviolet light, therefore allowing a 3D object to be built up layer by layer. However, the printed layers are not perfectly uniform and any irregularities can stack up, leading to defects in the resulting object. The problem is usually solved by levelling each layer using a roller or blade (not shown), but this limits the range of materials that can be used. Buchner *et al.*[1] address this problem using a machine-vision system (comprising four cameras and two laser sources) that scans the surface of each layer, mapping out the irregularities. **b**, The printer then deposits extra resin to fill in any gaps. **c**, This produces a smooth surface on which the next layer can be printed.

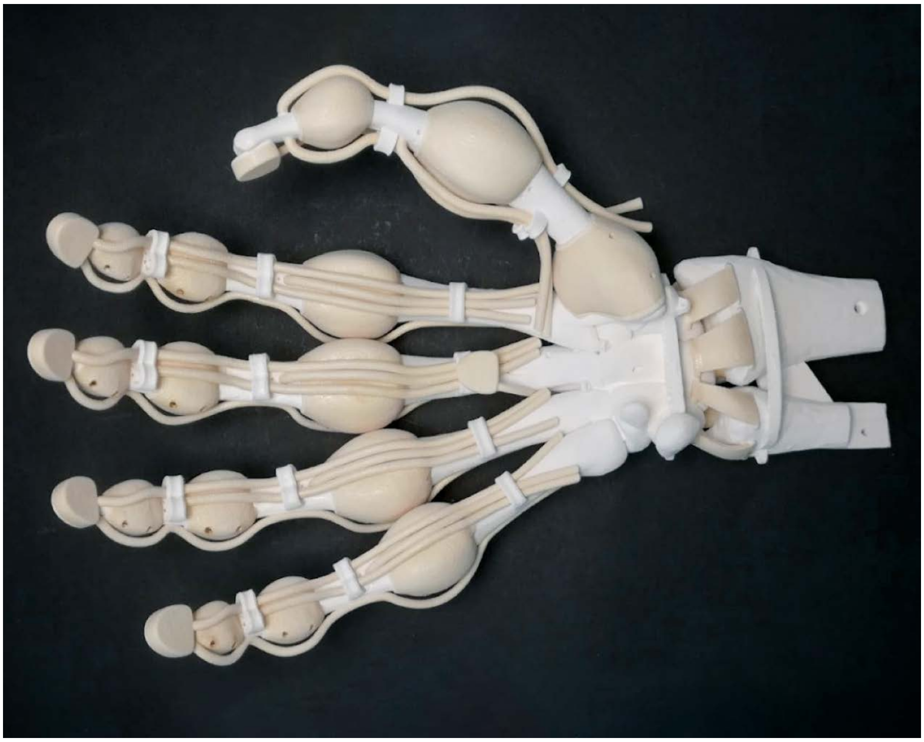

Figure 2 | A 3D-printed robotic hand. Buchner *et al.*[1] used their machine-vision-guided 3D printer to produce a robotic hand, which was printed using two different materials. The hand can be driven pneumatically to grasp objects in response to pressure applied at the fingertips.

commercially available inkjet 3D printers.

As a proof of concept, Buchner *et al.* 3D printed a tendon-driven hand composed of a rigid load-bearing core and a soft bendable shell (Fig. 2). This construct was embedded with channels that allow pneumatically driven movement, and was seamlessly integrated with membranes – printed in place at the fingertips – for measuring applied pressure. They also demonstrated that the hand could make a grasping action in response to the sensed pressure. Using a similar design, the authors constructed a multifunctional robot that can move, sense and grasp objects.

Buchner and colleagues also built a fluidic pump that resembles a biological heart. The construct was integrated with one-way valves, chambers, membranes and conduits, and could produce flow rates of up to 2.3 litres per minute. In another example, the authors printed metamaterials – constructs that have specially engineered substructures and properties that can surpass those of conventional materials[5]. Buchner *et al.* show that, by precisely modulating the dimensions of the soft links and rigid nodes of a truss-like metamaterial, they could tune the mechanical response of the metamaterial under compression.

Excitingly, these diverse examples were printed using just a few materials. Future work will no doubt expand the range of materials that can be printed, and thereby increase the functionalities of the resulting constructs – for example, by printing nanomaterials[6]. It should be noted, however, that the microscale nozzles needed for high-resolution printing can eject only inks that have a narrow range of fluidic properties. Further development of materials with customized chemistries will create more inks that have the desired properties.

Although the mechanical constructs reported in this work represent considerable advances in the complexity of multi-material integration, they still require external pneumatic pumps and electronics for movement and sensing. Buchner and colleagues' machine-vision system might help to lower the barrier to fabricating devices that incorporate commercially available components such as electronic chips and inkjet-printed electronics.

It might also aid the combination of other 3D-printing modalities with material jetting. For instance, printer modules that extrude viscous polymers could be integrated to enable the co-printing of components that provide movement capabilities[7,8], and extrusion printing of nanomaterials could allow co-fabrication of 3D electronic devices[9]. Other compatible fabrication methods could also be integrated – for example, electrospray deposition could be used to add a coating of biologically active molecules to surfaces[10,11]. In the meantime, Buchner *et al.* have demonstrated a powerful and inspirational example of how machine vision can overcome a fundamental limitation of an established 3D-printing technology, thereby enabling new multi-material 3D-printing capabilities.

From the archive

How to ventilate a prairie dog's burrow, and a bid to correct a large number of popular fallacies.

50 years ago

Prairie dogs (*Cynomys ludovicianus*) have a problem. These rodents live in long narrow burrows ... which must somehow be ventilated. Vogel, Ellington and Kilgore ... have calculated that, at the very least, there must be complete exchange of the air in the burrow with the atmosphere every 10 h and probably more often. They found that neither diffusion of oxygen through the soil or at the burrow entrance nor the direct action of the wind adequately explains how gas is exchanged with the atmosphere to meet the respiratory needs of the animal. How then do the prairie dogs avoid suffocation? Vogel *et al.* argue that two physical principles may underlie the ventilation ... Either mechanism demands that the two entrances to a burrow be dissimilar. Now it has been known for some time that prairie dogs do indeed build two sorts of entrance to their burrows: 'dome craters' (wide and rounded) and 'rim craters' (narrow, steep-walled, with a rim). But the functional significance of these two types was unknown.

From *Nature* 16 November 1973

100 years ago

Popular Fallacies Explained and Corrected (with Copious References to Authorities). By A. S. E. Ackermann — To every one who has made a special study of any branch of human knowledge there must, at some time or another, have come a feeling of surprise at the large number of errors which exist in the popular mind regarding ... presumably every ... subject. The previous editions of this book have proved of immense value in helping to correct the many errors which still persist in spite of the progress of popular education and the many devices now used for the dissemination of accurate information. A very real welcome is, therefore, assured for this the third edition ... The number of fallacies dealt with has been increased from 460 to 1350, and these cover practically every branch of human activity.

From *Nature* 17 November 1923

Yong Lin Kong is in the Department of Mechanical Engineering, University of Utah, Salt Lake City, Utah 84112, USA.
e-mail: yonglinkong@alumni.princeton.edu

1. Buchner, T. J. K. *et al. Nature* **623**, 522–530 (2023).
2. Zhu, Z., Ng, D. W. H., Park, H. S. & McAlpine, M. C. *Nature Rev. Mater.* **6**, 27–47 (2021).
3. Jin, Z., Zhang, Z., Demir, K. & Gu, G. X. *Matter* **3**, 1541–1556 (2020).
4. Sitthi-Amorn, P. *et al. ACM Trans. Graph.* **34**, 129 (2015).
5. Kadic, M., Milton, G. W., van Hecke, M. & Wegener, M. *Nature Rev. Phys.* **1**, 198–210 (2019).
6. Elder, B. *et al. Adv. Mater.* **32**, 1907142 (2020).
7. Skylar-Scott, M. A., Mueller, J., Visser, C. W. & Lewis, J. A. *Nature* **575**, 330–335 (2019).
8. Larson, N. M. *et al. Nature* **613**, 682–688 (2023).
9. Kong, Y. L. *et al. Nano Lett.* **14**, 7017–7023 (2014).
10. Park, S. H. *et al. Nature Commun.* **14**, 4896 (2023).
11. Kovacevich, D. A. *et al. ACS Appl. Mater. Interfaces* **12**, 20901–20911 (2020).

The author declares competing interests; see go.nature.com/47ervfk.

Microbiology

Viruses use RNA decoys to thwart CRISPR defences

Carolyn Kraus & Erik J. Sontheimer

Bacteria and archaea are microorganisms that often use RNA-guided defences called CRISPR to destroy the genomes of viruses that infect them. It now emerges that viruses make RNAs that act as mimics to divert such defences. **See p.601**

Microorganisms such as bacteria and archaea flourish despite the ubiquitous presence of viruses, which are called bacteriophages or phages, that can infect them. This resilience is partly due to the evolution of anti-phage defence systems that thwart viral infection[1]. On page 601, Camara-Wilpert *et al.*[2] uncover a previously unknown strategy that viruses use to divert antiviral defences down a dead-end path.

Prominent among anti-phage systems are what are termed adaptive immune pathways. These depend on genetic sequences called CRISPRs, which produce CRISPR RNA (crRNA) sequences that act as guides to direct the destruction of corresponding phage genomes[3]. In an ancient arms race that continues to this day, phages have in turn evolved countermeasures, such as Acr proteins, which function as anti-CRISPRs by jamming the CRISPR machinery and subverting anti-phage defences[4].

CRISPR regions of the genome include arrays of unique 'spacer' sequences, which are derived from the genomes of previously encountered phages. These spacers are separated from each other by short repeat sequences (Fig. 1a). The crRNAs produced from these CRISPR sites consist of a single spacer sequence flanked on one or both sides by portions of the repeats. CRISPR sites are generally accompanied in adjacent genome sequences by genes encoding Cas proteins, which assemble into crRNA-guided complexes that home in on matching sequences in the genomes of attacking phages.

Many categories of CRISPR–Cas systems (types I–VI) have been defined, and nearly all have been found to be susceptible to inhibition by more than one Acr protein. At least 100 Acr families have been identified[5], and these have a remarkable diversity in their structures, mechanisms and specificities for the subsets of CRISPR systems that they inhibit[6]. Most Acrs investigated thus far recognize and bind to Cas proteins and interfere with their interactions, structural transitions or other biochemical activities. Phages have been known to co-opt entire CRISPR–Cas systems for their own purposes, such as interference with other viruses during the infection of a microbe by more than one competing phage[7].

Occasionally, other CRISPR-like sequences known as solitary repeat units (SRUs) – each with only one spacer and one repeat – can be found in the genomes of phages and other mobile genetic elements (MGEs), such as a type of circular DNA called a plasmid. Strangely, unlike most viral CRISPR arrays, these SRUs are generally not accompanied by genes encoding Cas proteins. Camara-Wilpert and colleagues set out to explore the roles of these SRUs and test the hypothesis that they have anti-CRISPR functions.

To determine whether SRUs can protect phages from CRISPR-mediated interference, the authors identified an SRU with similarities to the crRNAs encoded by their chosen host bacterial strain and incorporated the SRU into that strain of bacterium. After finding that the SRU expressed small crRNA-like RNAs, the authors infected bacteria with a phage that is normally targeted and suppressed by the host bacterium's type I-F CRISPR–Cas system. Importantly, the authors found that, relative to their non-SRU-containing counterparts, SRU-expressing bacteria were much more susceptible to phage infection and

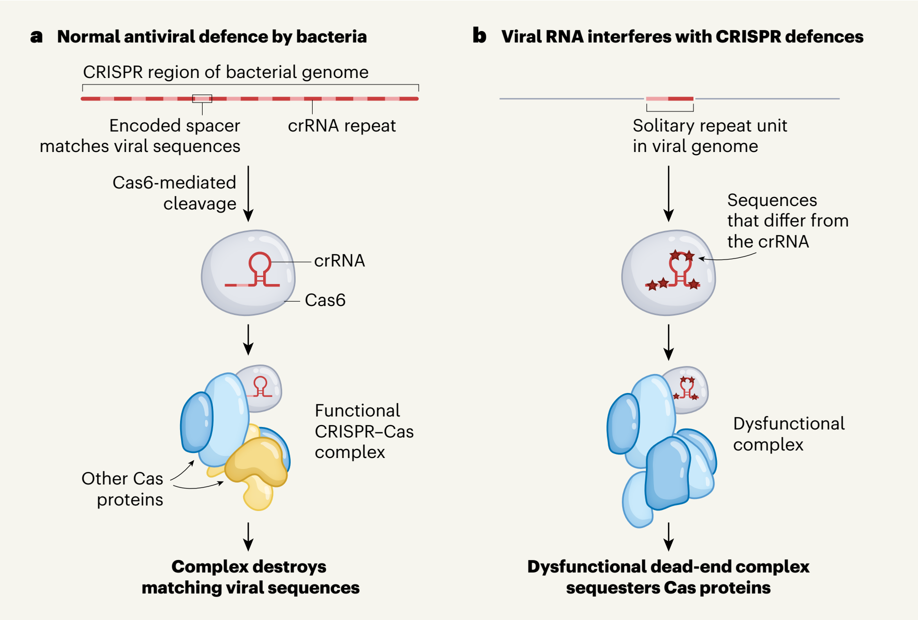

Figure 1 | How viruses combat a bacterial defence. a, Some bacteria use a type of defence that depends on what are called CRISPR sequences, encoded in the bacterial genome. These contain repeat sequences and spacer sequences that correspond to CRISPR RNAs (crRNAs), which match viral sequences. These sequences are cleaved by the enzyme Cas6 and form a complex with other Cas proteins that can destroy viral genomes. **b**, Camara-Wilpert *et al.*[2] reveal that some viruses can thwart such antiviral defences by encoding sequences called solitary repeat units that are similar to, but distinct from, segments of functional CRISPR sequences. The solitary repeat unit is cleaved by Cas6 and forms a dysfunctional complex with a subset of the usual Cas proteins.